Information Sciences Letters
An International Journal

http://dx.doi.org/10.18576/isl/130215

A Framework for Studying the Possibility of Using Basalt Cement as a Cladding Material for Indoor Spaces

H. A. Saudi[1,], Maha F. A. Anber[2], Ahmed. M. Mabrouk[3] and Algendy S. Algendy[3]*

[1]Physics Department, Faculty of Science, Al-Azhar University (girls branch), Cairo, Egypt
[2]Architectural Engineering Department, Higher Institute of Engineering, El-Shorouk Academy, Cairo, Egypt
[3]Architecture Department, Faculty of Engineering, Al-Azhar University, Nasr City, Cairo, Egypt

Received: 22 Feb. 2023, Revised: 12 Mar 2023, Accepted: 22 May 2023
Published online: 1 Mar. 2024

Abstract: The indoor environment affects the quality of life, well-being, and productivity. Indoor occupants are affected by multiple factors such as heat, acoustics, lighting, and electromagnetic radiation. Therefore, cement mixed with basalt rocks was prepared and the effect of electromagnetic radiation on it was studied. It was clear from the results that cement mixed with basalt rocks is good at mitigating radiation and absorbing heat from the internal environment. Therefore, it is possible to use cement mixed with basalt as an internal cladding material to protect against the danger of radiation in enclosed spaces.

Keywords: Indoor environmental quality; radiation protection; cement-based composites.

1 Introduction

The usage of high-tech equipment by individuals, such as smartphones, computers, and televisions, has now become a necessary and a prerequisite of this era's requirements to give comfort and complete work more quickly. However, using these cutting-edge tools could expose users to certain possible drawbacks. Numerous recent research has demonstrated that electromagnetic radiation from modern workplaces and home electronics is a source of radioactive contamination and that it can have negative health effects [1, 2]. Radiation protection should be considered from the standpoint of health issues to sustain human well-being [3].

Factors that have an impact on how people live within buildings serve as a representation of indoor environmental quality. According to Holmgren M et al., indoor environmental quality in businesses enhances employees' physical and emotional well-being, which raises productivity. [4]. The raw material basalt stone has a variety of benefits, including thermal insulation, fire resistance, excellent durability, and resistance to water and moisture. This substance has the potential to be employed as cladding for indoor construction.

To investigate its qualities, this research prepares and evaluates a cement-based composite. The investigation of how gamma radiation interacts with matter is an essential subject in the domains of nuclear medicine, diagnostics, radiation protection, radiation physics, and radiation chemistry. The probability of radiation interacting with a material per unit length is known as the linear attenuation coefficient (μ), which has a substantial effect on radiation shielding. The mass attenuation coefficient (m), which is determined as the substance's per unit mass, is the primary physical parameter that describes how gamma rays diffuse and penetrate through materials.

Understanding (m), (t), (el), the effective atomic number Zeff, and the effective electron number Neff is crucial because gamma radiation scattering, and absorption are associated with the density and atomic number of the material [5]. Ionizing radiation has been used in medicine to treat and manage malignant tumors using X-rays and high-energy gamma rays. The benefits and risks of this radiation are known to humans. Traditional blocks and multi-leaf collimators (MLCs) have been made from high atomic number (High-Z) materials to produce better beams and reduce the radiation absorbed by healthy tissue. As one of the most popular materials used for radiation shielding in nuclear reactors and radiation therapy centers, as well as for limiting radiation leakage from radioactive sources, in concrete, lead (Pb) is currently the most widely used material due to its high atomic number (Z), low cost, and availability [6]. It is a cheap substance with a big capacity for mixing a lot of secondary source materials and trash [7].

To replace potentially dangerous cementitious composites with lead with environmentally friendly materials like basalt, extensive research is being conducted in this area. The most common form of basalt, a dark-colored, fine-grained volcanic rock, is the boulder. It is frequently utilized as an aggregate in construction projects after being crushed. More

*Corresponding author e-mail: Heba_Saudi@azhar.edu.eg

than 50% of the compounds in basalt rocks are oxides of silicon (SiO2), with the remainder being oxides of aluminum (Al2O3), iron (Fe2O3), magnesium (MgO), calcium (Ca), sodium (Na), and potassium (K2O) [8] [9]. The most hazardous greenhouse gas in the world, carbon dioxide, can be absorbed and converted by basalt into solid rocks or stones that dissolve within the basalt's internal components. This decrease in the amount of carbon dioxide in the Earth's atmosphere causes an increase in global temperature [6].

The balance of energy resources required to support economic growth in both the industrialized and developing globe must include cheap and plentiful fossil fuels. On the other hand, large cuts in carbon dioxide emissions are needed to mitigate the impacts of climate change caused by rising atmospheric carbon dioxide concentrations. [7]. Therefore, the manufacturing of Portland cement grafted with various proportions of basalt was taken into consideration to close the gap between the necessity of using fossil fuels and the reduction of carbon dioxide emissions at the same time to protect the environment and slow down global warming.

Based on the review of the literature, it can be believed that there have been few or few recent scientific findings regarding the effects of basalt powders, and further study is necessary to fully comprehend how basalt particle size and content affect the structural, physical, mechanical, radiological, and carbon absorption properties of concrete protection.

Basalt stones exist widely in Egypt; which encourages to use of basalt in creating carbon absorbent materials; This urged the researcher to find a way to exploit basalt in the built environment and use it as a cladding material for indoor spaces; to reduce the carbon emissions, Figure1 explains some of basalt quarries in Egypt.

This study aims to conduct a comprehensive experimental evaluation of the effect of cement mixed with basalt on the gamma-ray shielding properties.

Fig. 1: explains some of the basalt quarries in Egypt.

2 Materials and Methods

2.1. Materials

CEM cement paste was manufactured using Portland cement and tap water, as this type of cement has many advantages, including very practical, and it has a gradual increase in its initial strength, its density is rather high compared to other types, as in Table 1, in addition to its high resistance to chemical reactions. Table 1 gives us Information about the chemical composition of cement and the proportion of each compound within it.

Table 1: Chemical compositions of Portland cement [wt.%]

Material	**CaO**	**SiO_2**	**Al_2O_3**	**Fe_2O_3**	**MgO**	**Na_2O**	**K_2O**	**Loss on ignition**	**Specific Density (g/cm^3)**
CEM	63.1	17.7	6.2	4.4	1.8	0.1	0.9	3.05	3.11

Basalt rock extracted from nature was used and crushed for two hours to obtain it in powder form. Then, it was added to the production of cement paste with a fixed ratio of water and different proportions of basalt. As indicated in Table 2, five series of mixed cement pastes with basalt contain 0, 5, 10, 15, and 20 by weight. Using a lab mill, grinding was carried out as follows: first, gradual grinding for 25 seconds; second, quick grinding. By utilizing toluene as the immersion fluid in the Archimedes technique, the density (ρ) of the prepared samples was measured.

Table 2: Design of basalt cement paste mixture.

Paste	Cement [g]	Water [g]	Basalt particles [g]
CB0	1000	400	0
CB5	950	400	50
CB10	900	400	100
CB15	850	400	150
CB20	800	400	200

2.2. Measurement of radiation attenuation coefficients

Gamma-ray attenuation tests were performed using a proprietary technique and the use of a beam collector to minimize the scattering of photons back into the detector, eliminating the need for accumulation correction. Figure 2 depicts the actual experimental setup for gamma-ray attenuation measurements. For varying photon energies, radioactive sources with an activity of ten mega each were used: 133Ba, 60Co, 137Cs, and 232Th. Each image peak was received between 102 and 104 counts, which were recorded at the specified count time. The arrangement uses a 2-cm collimator for gamma-ray shielding. Figure 2 depicts the actual experimental setup for gamma-ray attenuation measurements.

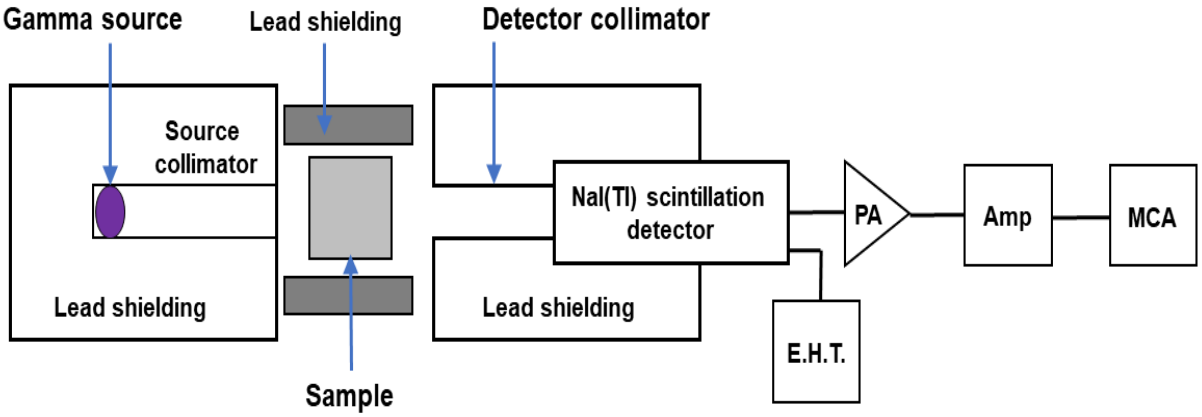

Fig. 2: Experimental configuration for Gamma radiation attenuation measurement.

Measurement was made using gamma radiation lines with energies of 80, 356, 662, 911, 1173.23, and 1332.49 keV, generated by standard radioactive sources 131Ba, 137C, and 60Co, to determine the attenuation coefficients of basalt cement putty samples. The detection system energy and efficiency calibration also used these standard sources. Beer's law was applied to the measured incident (I0) and transmitted (I) photon intensity to calculate the linear attenuation coefficient values, (Eq. 1) [8, 9, 1]:

$$\mu = \frac{1}{t} ln(\mathrm{I}/Io) \quad (1)$$

where is the material thickness (in cm).

Since the density of the attenuation is medium, the value also depends on the state of the substance (solid, liquid, or gaseous). Therefore, in the shielding analysis, the linear attenuation coefficient

is chosen to be normalized per unit intensity, μ/ρ(cm2/g), is chosen. (Eq. 2).

$$\mu/\rho = \frac{1}{x} ln(\mathrm{I}/Io) \quad (2)$$

where x is the sample mass thickness (cm2/g) [9,10].

3 Results and discussion

Figure 3 shows the current values of the density and depicts their relationships with the Concentration of basalt cement paste mixture. The density increases by adding basalt to the cement. The increase in density is because the basalt contains[11] more than 10% iron oxide, which has a higher density, as well as 17% aluminum oxide compared to Portland cement.

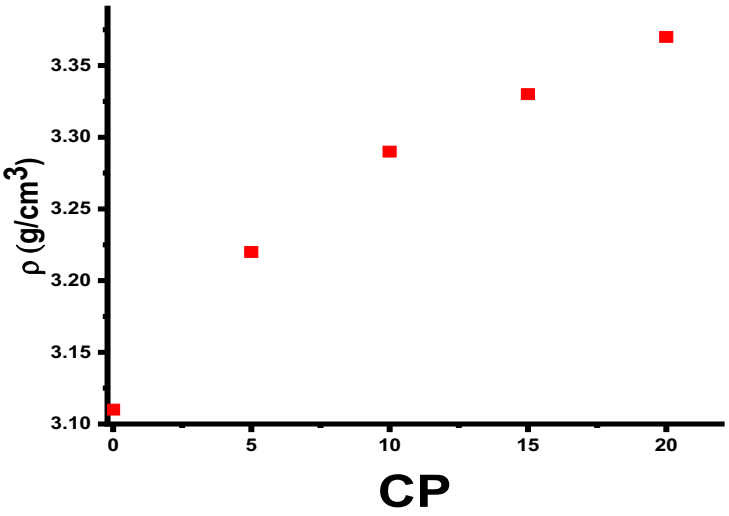

Fig. 3: Density of different concentrations of basalt cement paste mixture (wt%).

Vertical narrow beam geometry was used to determine the linear attenuation coefficient of basalt cement paste, as illustrated in Figure 2. As shown in Figure 4, for example, I and I0 represent the gamma radiation intensity of energy E that is measured using a container with and without a thickness of t. We then calculate the linear attenuation coefficient () from the slope, and the mass (/) attenuation coefficients using the density. Table 3 displays the experimental values for the linear attenuation coefficient. Naturally, when basalt content rises, so do the linear attenuation coefficients. Basalt includes FeO, which likewise has the property of attenuating radiation, which may explain this behavior. With an increase, the linear attenuation declines. [12, 13]. The interaction of photons with various concentrations of basalt cement paste mixture can be used as an explanation for photoelectricity, Compton scattering, and pair generation mechanisms. The photoelectric effect has a higher attenuation factor at low energy than other effects. Based on the Compton effect's attenuation coefficient [14,15,16]. Figure 5 displays the mass attenuation coefficients (MAC) values from an experimental and theoretical study for the incident gamma, the thing that prevents photoelectricity from working. Half-value layer thickness (HVL) is a parameter for the attenuation coefficient. It alludes to the 50% reduction in radiation intensity caused by the material thickness. Table 4's measured HVL values demonstrate that thinner layers were needed since pastes with higher basalt concentrations had lower HVL. [13,14]. For the incident gamma energy range (10-3 MeV - 105 MeV), experimental and theoretical results of mass attenuation coefficients (MAC) values are displayed in Fig. 5. The experimental result and the calculated data by XCOM and PHY-X are in good agreement, as shown in Fig. 5. Furthermore, an abrupt peak occurs, and the MAC values drop with an increase in energy up to 0.1 MeV. Figure 5 shows that the composition of the samples of basalt cement paste mixture and the energy of the -photon are the two key determinants of MAC values. In the low energy zone, all compositions have relatively high MAC values. As the basalt ratio rises, the MAC value rises as well. Based on the predominance of the photoelectric phenomena, where the cross-section of this interaction largely depends on the atomic number, the high values of the MAC in the low energy zone may be established. Furthermore, due to the dominance of Compton scattering in this zone, MAC values at intermediate energy (energy greater than 1022 keV) fluctuate for all samples within a small range and exhibit less energy-dependent behavior. Additionally, there is a weak relationship between MAC and the chemical makeup of the samples. Due to the pair production process supremacy at high energies, MAC values are nearly constant, and the attenuation behavior becomes consistent across all samples.

To examine the shielding efficiency of the basalt cement, paste mixture system, the results of the MAC were compared with those of another shielding material such as concrete. The chosen concrete types are ordinary concrete, barite concrete, and iron concrete. The concrete densities and MAC values at 0.662 MeV are given in Table 5 [18, 19]. Fig. 6 shows that the basalt cement paste mixture system has higher MAC values than that of the three concrete types. These

findings demonstrate that the basalt cement paste mixture in the current study has an adequate level of -photon shielding efficacy. The effective atomic number (Zeff) plays a major role in the evaluation of the energy-related variable as an alternative material [20, 21]. Gamma-ray absorption, for example, depends on the composite's Zeff and photon energy. The attenuation characteristics of the materials are assessed using the Zeff parameter. The Zeff is a measure of the percentage of sample electrons involved in photon-atom interactions. Utilizing the Phy-X/PSD and WinXcom programs, the Zeff for the examined basalt cement paste combination was assessed. Fig. 7 depicts the variations in Zeff values of all investigated basalt cement paste mixtures with photon energies ranging from 0.05 to 10 MeV. According to Figure 7, the mixture of basalt cement paste and Zeff has the highest photon energy values, E 0.1 MeV (i.e., the photoelectric zone). The Zeff fluctuations were negligible and attained their smallest values in the energy range between 0.4 and 3 MeV (Compton scattering). Additionally, for high gamma photon energies greater than 3 MeV, when pair production is predominant, there is a modest increase in the Zeff values. the effective electron density or effective electron number per unit mass, [20, 23] The change of Neff values with photon energy as Zeff, where Neff is directly proportional to Zeff, showed similar behavior. The Neff varies abruptly with photon energy, as seen in Fig. 8, and abrupt leaps in the low energy area are connected to the photoelectric absorption edge. In addition, when pair creation increasingly takes over as the primary interaction mechanism, the Neff rapidly declines with photon energy increase and begins to climb with a slight slope above 3 MeV.

When compared to other areas, the region where photoelectric absorption dominates has a higher rate of free electron generation. The photons in this range are more likely to interact with target material electrons because they have lower energy and longer wavelengths [24]. Due to the high probability, more photons are absorbed by electrons, producing more free electrons.

When compared to other areas, the region where photoelectric absorption dominates has a higher rate of free electron generation. The photons in this range are more likely to interact with target material electrons because they have lower energy and longer wavelengths[24]. Due to the high probability, more photons are absorbed by electrons, producing more free electrons.

The neutron is particularly significant since it is uncharged, interacts only with atomic nuclei results in indirect ionization, and has a greater capacity for penetrating materials. The attenuation notion describes how well a substance can guard against neutrons. The macroscopic effective removal cross-section is one characteristic that affects neutron attenuation [25, 26]. Using fast neutron removal cross-sections, the basalt cement paste's effectiveness as a neutron shield was assessed. (ΣR). Phy-X software was used to estimate the fast neutron effective removal cross-section values for the basalt cement pastes system. Fig. 9 represents the calculated ΣR values of basalt cement pastes at different ratios. The ΣR values slightly increase with the basalt content because the ΣR of basalt is higher than that of cement. Therefore, when basalt cement pastes are utilized for shielding against gamma and neutron rays, the glass density must be taken into consideration.

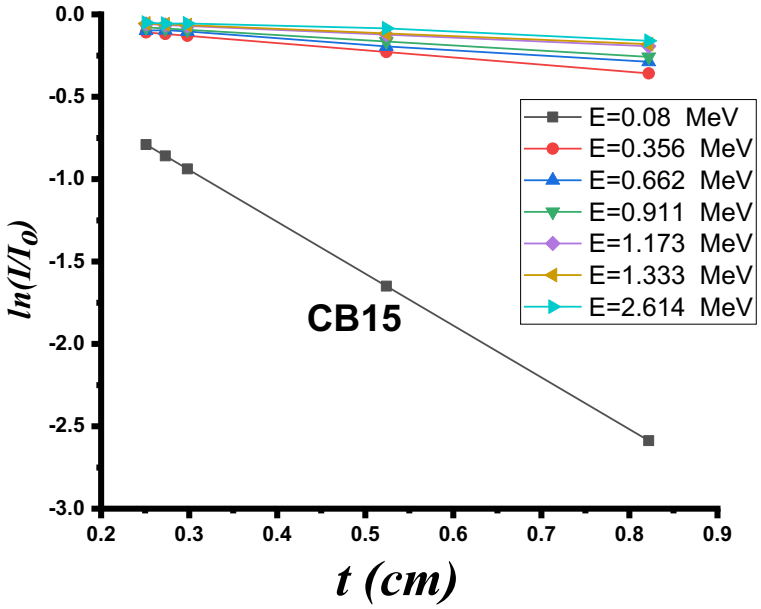

Fig. 4: Plot of I/Io Vs thickness t for CB15 at different energies

Table 3: Experimental linear attenuation coefficients with the gamma photon energy of basalt cement pastes

Paste	Energy (MeV)						
	0.08	0.356	0.662	0.911	1.173	1.333	2.614
CB0	0.859	0.383	0.245	0.215	0.187	0.168	0.126
CB5	1.419	0.546	0.292	0.251	0.221	0.21	0.151
CB10	1.948	0.679	0.318	0.272	0.234	0.221	0.159
CB15	1.969	0.837	0.349	0.293	0.249	0.237	0.169
CB20	2.845	1.02	0.377	0.317	0.27	0.261	0.173

Table 4: The experimental HVL (in cm) of basalt cement pastes with experimental errors of less than 5%.

Sample name	**HVL (cm)**						
	0.08 MeV	0.238 MeV	0.662 MeV	0.911 MeV	1.173 MeV	1.333 MeV	2.614 MeV
CB0	0.84	1.79	2.73	3.18	3.69	3.89	5.49
CB5	0.52	1.24	2.33	2.68	3.11	3.38	4.69
CB10	0.38	1.16	2.14	2.53	2.9	3.15	4.41
CB15	0.33	0.81	1.93	2.41	2.72	2.91	4.11
CB20	0.18	0.63	1.79	2.21	2.53	2.75	3.84

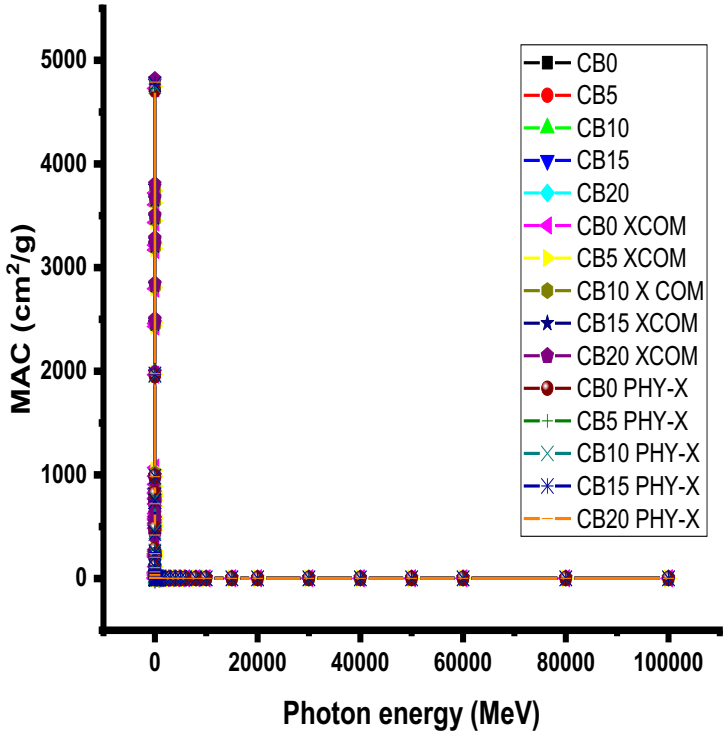

Fig. 5: Experimental, XCOM, and PHY-X MAC values versus the incident photon energy in range (10-3 MeV - 1.5 MeV).

Table 5: The chemical composition of ordinary concrete [4][5]

Material	**Density (g/cm³ 662 KeV at**	**MAC (cm²/g)**
Ordinary concrete	**2.3**	**0.0778**
Barite concrete	**3.5**	**0.078**
Iron Concrete	**4.5**	**0.0777**

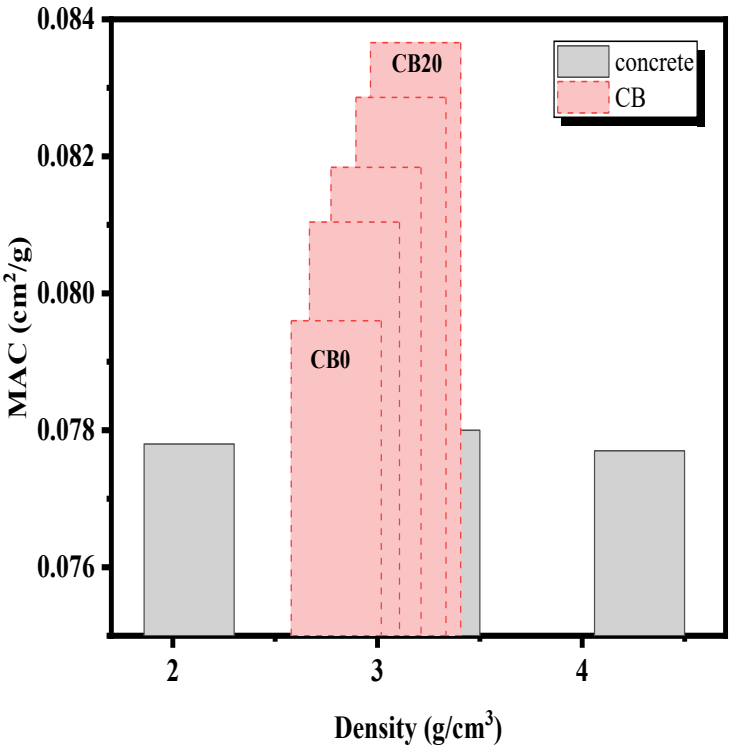

Fig. 6: An experimental MAC value of basalt cement pastes compared with concrete density.

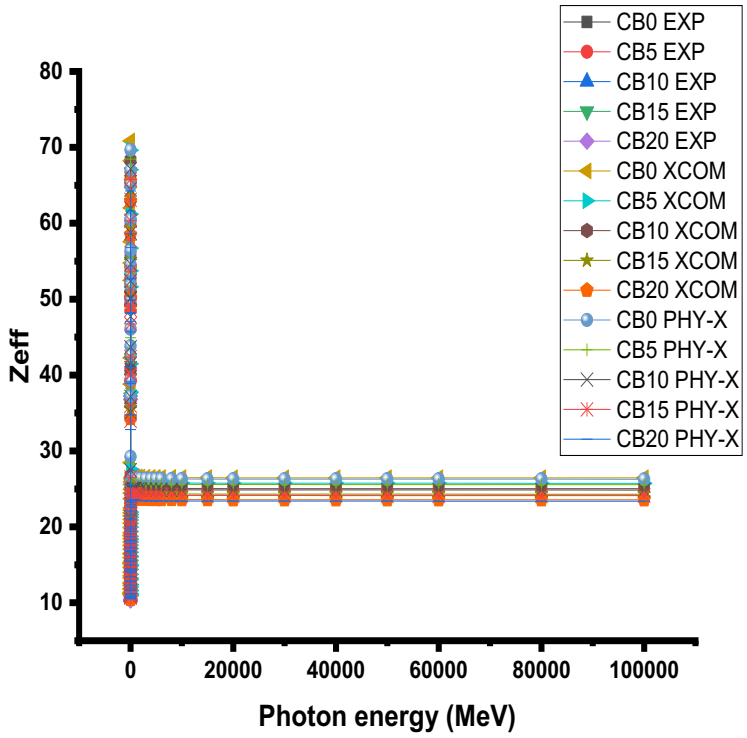

Fig. 7: Zeff dependence on γ energy of basalt cement pastes system

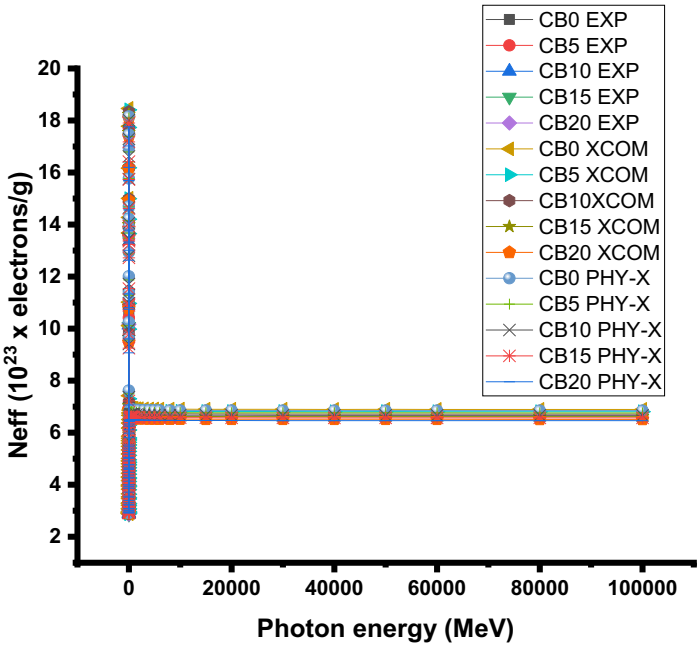

Fig. 8: Neff dependence on γ energy of basalt cement pastes system

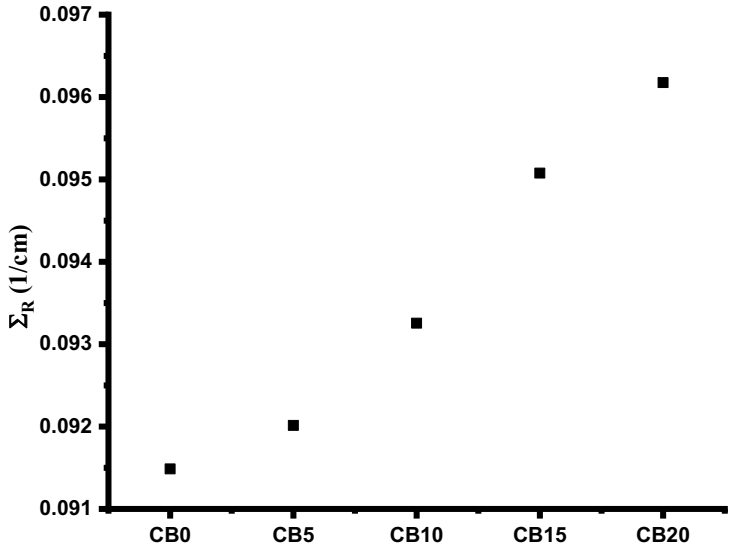

Fig. 9: ΣR values of basalt cement pastes system

4 Conclusions

The outline of the study is summarized in the composition of basalt cement. The intensity and attenuation coefficients, respectively, were considered while calculating the study coefficients. The attenuation coefficients were seen to decrease while the average layer thickness increased with increasing basalt concentration. Multiple factors affect the quality of life and well-being of people in indoor spaces, such as heat, acoustics, lighting, electromagnetic radiation (radio waves, gamma rays, neutron, visible light, and X-rays), and many other factors that greatly affect their performance and productivity resulting from the use of electricity in buildings for electrical appliances and equipment. The results proved that basalt cement as a cladding material for indoor spaces provides protection from radiation

hazards and reduces the temperature in indoor spaces, especially with the increase in the percentage of basalt.

5 Declarations

Ethical Approval: Authors declare that this manuscript is original, has not been published before, and is not currently being considered for publication elsewhere.

Consent to participate: Not applicable.

Consent to publish: Not applicable.

Data availability: All data generated or analysed during this study are included in this publication.

Conflicts of Interest Statement

The authors certify that they have NO affiliations with or involvement in any organization or entity with any financial interest (such as honoraria; educational grants; participation in speakers' bureaus; membership, employment, consultancies, stock ownership, or other equity interest; and expert testimony or patent-licensing arrangements), or non-financial interest (such as personal or professional relationships, affiliations, knowledge or beliefs) in the subject matter or materials discussed in this manuscript.

References

[1] H. A. Saudi and S. U. E. Kameesy, "Effect of barium addition and plasma nitriding treatment on chemical and physical properties of Al, Pb borate glass system as a developed radiation shield," J. Phys. Conf. Ser., vol. 1253, no. 1, 2019, doi: 10.1088/1742-6596/1253/1/012033.

[2] Z. O. I. Alhekail, "Electromagnetic Radiation from Microwave Ovens," Journal of Radiological Protection, Vol. 21, No. 3, 2001, pp. 251-258. doi:10.1088/0952-4746/21/3/303.

[3] E. VanWijngaarden, D. A. Savitz, R. C. Kleckner, J. Cai, and D. Loomis, "Exposure to Electromagnetic Fields and Suicide among Electric Utility Workers: A Nested Case—Control Study," Occupational Environmental Medicine, Vol. 57, No. 4, 2000, pp. 258-263. doi:10.1136/oem.57.4.258.

[4] Tingting Fu, Yu Chen, Lingli Han, Qizhong Qin, Preliminary Report on the Indoor Electromagnetic Radiation in a Municipality of Western P.R. China: Up-to-Now Still within the Range, Journal of Electromagnetic Analysis and Applications, 2012, 4, 199-205.

[5] Holmgren M, Kabanshi A, Sörqvist P. Occupant perception of 'green' buildings: Distinguishing physical and psychological factors. Building and Environment. 2017;114:140-147.

[6] S. S. Obaid, D. K. Gaikwad, and P. P. Pawar, "Determination of gamma-ray shielding parameters of rocks and concrete," Radiat. Phys. Chem., vol. 144, pp. 356–360, Mar. 2018, doi: 10.1016/j.radphyschem.2017.09.022.

[7] P. Sikora, A. M. El-Khayatt, H. A. Saudi, S. Y. Chung, D. Stephan, and M. Abd Elrahman, "Evaluation of the effects of bismuth oxide (Bi2O3) micro and nanoparticles on the mechanical, microstructural and γ-ray/neutron shielding properties of Portland cement pastes," Constr. Build. Mater., vol. 284, p. 122758, 2021, doi: 10.1016/j.conbuildmat.2021.122758.

[8] H. M. Gomaa, H.A. Saudi, I.S. Yahia, M.A. Ibrahim, H.Y. Zahran, Influence of exchanging CeO2 with Cu2O3 on both structural matrix, shielding, and linear/nonlinear optical parameters of the cerium-sodium borate glass, Optik (Stuttg). 249 (2021) 168267. https://doi.org/10.1016/j.ijleo.2021.168267.

[9] G. A. Khater, H.A. Saudi, Glass and Glass-Ceramics Based on Weathered Basaltic Rock for Radiation Shielding Applications, (2021).

[10] Y. B. Saddeek, K.H.S. Shaaban, R. Elsaman, A. El-Taher, T.Z. Amer, Attenuation-density anomalous relationship of lead alkali borosilicate glasses, Radiat. Phys. Chem. 150 (2018) 182–188. https://doi.org/10.1016/j.radphyschem.2018.04.028.

[11] R. Picha et al., "Gamma and neutron attenuation properties of the barite-cement mixture," J. Phys. Conf. Ser., vol. 611, no. 1, 2015, doi: 10.1088/1742-6596/611/1/012002.

[12] M. Y. Hassaan, A. G. Mostafa, M. A. Ahmed, H. M. H. Saad, and H. A. Saudi, "DC and AC Conductivity Study of Basalt Glasses Containing High Concentrations of Na+Ions," Silicon. 2018.

[13] B. P. McGrail, H. T. Schaef, A. M. Ho, Y. J. Chien, J. J. Dooley, and C. L. Davidson, "Potential for carbon

dioxide sequestration in flood basalts," J. Geophys. Res. Solid Earth, vol. 111, no. 12, 2006, doi: 10.1029/2005JB004169.

[14] H. A. Saudi and S. U. E. Kameesy, "Effect of barium addition and plasma nitriding treatment on chemical and physical properties of Al, Pb borate glass system as a developed radiation shield," J. Phys. Conf. Ser., vol. 1253, no. 1, 2019, doi: 10.1088/1742-6596/1253/1/012033.

[15] H. M. Gomaa, H.A. Saudi, I.S. Yahia, M.A. Ibrahim, H.Y. Zahran, Influence of exchanging CeO2 with Cu2O3 on both structural matrix, shielding, and linear/nonlinear optical parameters of the cerium-sodium borate glass, Optik (Stuttg). 249 (2021) 168267. https://doi.org/10.1016/j.ijleo.2021.168267.

[16] G.A. Khater, H.A. Saudi, Glass and Glass-Ceramics Based on Weathered Basaltic Rock for Radiation Shielding Applications, (2021).

[17] Y. B. Saddeek, K.H.S. Shaaban, R. Elsaman, A. El-Taher, T.Z. Amer, Attenuation-density anomalous relationship of lead alkali borosilicate glasses, Radiat. Phys. Chem. 150 (2018) 182–188. https://doi.org/10.1016/j.radphyschem.2018.04.028.

[18] A. Mesbahi, H. Ghiasi, Shielding properties of the ordinary concrete loaded with micro- and nano-particles against neutron and gamma radiations, Appl. Radiat. Isot. 136 (2018). https://doi.org/10.1016/j.apradiso.2018.02.004.

[19] E. S. A. Waly, M.A. Bourham, Comparative study of different concrete composition as gamma-ray shielding materials, Ann. Nucl. Energy. 85 (2015). https://doi.org/10.1016/j.anucene.2015.05.011.

[20] S. Stalin, D.K. Gaikwad, M.S. Al-Buriahi, C. Srinivasu, S.A. Ahmed, H.O. Tekin, S. Rahman, Influence of Bi2O3/WO3 substitution on the optical, mechanical, chemical durability and gamma-ray shielding properties of lithium-borate glasses, Ceram. Int. 47 (2021) 5286–5299. https://doi.org/10.1016/j.ceramint.2020.10.109.

[21] H. O. Tekin, G. Susoy, S.A.M. Issa, A. Ene, G. ALMisned, Y.S. Rammah, F.T. Ali, M. Algethami, H.M.H. Zakaly, Heavy metal oxide (HMO) glasses as an effective member of glass shield family: A comprehensive characterization on gamma-ray shielding properties of various structures, J. Mater. Res. Technol. 18 (2022) 231–244. https://doi.org/10.1016/j.jmrt.2022.02.074.

[22] S. A. M. Issa, A. Kumar, M.I. Sayyed, M.G. Dong, Y. Elmahroug, Mechanical and gamma-ray shielding properties of TeO2-ZnO-NiO glasses, Mater. Chem. Phys. 212 (2018) 12–20. https://doi.org/10.1016/j.matchemphys.2018.01.058.

[23] D. ŞEN BAYKAL, H. TEKİN, R.B. ÇAKIRLI MUTLU, An Investigation on Radiation Shielding Properties of Borosilicate Glass Systems, Int. J. Comput. Exp. Sci. Eng. 7 (2021) 99–108. https://doi.org/10.22399/ijcesen.960151.

[24] L. Demir, I. Han, Mass attenuation coefficients, effective atomic numbers and electron densities of undoped and differently doped GaAs and InP crystals, Ann. Nucl. Energy. 36 (2009) 869–873. https://doi.org/10.1016/j.anucene.2009.03.015.

[25] H. A. Sallam, H.A. Saudy, The Role of Replacing CdO by Fe 2 O 3 on the Fast Neutron Removal Cross Sections in Cd-Boro Phosphate Glass Shield, 2013 (2013) 3–7.

[26] G. Almisned, H.O. Tekin, H.M.H. Zakaly, S.A.M. Issa, G. Kilic, H.A. Saudi, M. Algethami, A. Ene, Fast neutron and gamma-ray attenuation properties of some hmo tellurite-tungstate-antimonate glasses: Impact of sm3+ ions, Appl. Sci. 11 (2021). https://doi.org/10.3390/app112110168.